

https://doi.org/10.1070/QEL16285

Influence of induced colour centres on the frequency–angular spectrum of a light bullet of mid-IR radiation in lithium fluoride

S.V. Chekalin, V.O. Kompanets, A.E. Dormidonov, V.P. Kandidov

Abstract. **The influence of the occurrence of a structure consisting of long-lived colour centres, formed in an LiF crystal upon filamentation of femtosecond mid-IR radiation, on the supercontinuum characteristics is investigated. With an increase in the number of incident pulses, the length and transverse size of the structure of colour centres induced in LiF increase, and the supercontinuum spectrum in the short-wavelength region is markedly transformed due to the occurrence of the waveguide propagation regime, absorption, and scattering of radiation from the newly formed structure of colour centres. Under these conditions, the intensity of the anti-Stokes wing decreases by two orders of magnitude after several tens of pulses. Spectral components arise in the visible range, the angular divergence of which increases with increasing wavelength.**

Keywords: *filamentation, femtosecond pulses, light bullets, supercontinuum, colour centres, LiF.*

1. Introduction

Fluorides of alkali metals, which are transparent in the range from UV to IR, are promising materials for supercontinuum generation under filamentation of femtosecond radiation. A particular place among them is occupied by the LiF crystal, which is characterised by the widest transparency range and band gap (about 14 eV) among all transparent dielectrics [1]. Specifically this material exhibited the most significant broadening of supercontinuum spectra to the UV region under femtosecond filamentation [2–4]. In addition, LiF is characterised by high thermal and optical stability, is less hygroscopic, and has properties facilitating its mechanical treatment in comparison with many other alkali halide crystals.

An important feature of this material is that long-lived colour centres (CCs) can be formed in it under high-power laser irradiation; these centres lead to a change in the refractive index in the range from UV to mid-IR and to the occurrence of absorption bands [1]. The colouring can be caused by (i) nonlinear photoexcitation of the LiF electron subsystem with the formation of excitons and electron–hole pairs by plasma during avalanche, tunnel, and multiphoton ionisation and (ii) direct excitation of excitons [5–7].

The decay of excitons and electron–hole pairs leads to the formation of elementary F centres (an F centre is a single anion vacancy with a captured electron) [8]. After the aggregation of a certain number of anion vacancies and nonluminescent F centres, luminescent aggregate CCs are formed (in particular, F_2 and F_3^+ CCs). These are dyads and triads of anion vacancies in neighbouring lattice sites with a captured pair of electrons, exhibiting luminescence peaks near wavelengths of 650 and 550 nm, respectively [1]. The processes of their formation in alkali halide crystals have characteristic times on the order of several picoseconds or more [9]; therefore, they occur after the transmission of femtosecond laser pulse and do not affect the supercontinuum formation under filamentation in the single-pulse regime.

The aforementioned CCs have such a strong luminescence that the long-lived structures consisting of them, formed by a single laser pulse, can easily be detected upon subsequent illumination into their absorption band near 450 nm by a cw laser (laser-induced colouration method) [10]. This circumstance made it possible to observe for the first time the formation of light bullets (LBs) with a duration close to that of one light field oscillation under single-pulse filamentation of pulses in the mid-IR region [i.e., in the region of anomalous group-velocity dispersion (GVD)] in the LiF crystal [11, 12]. In contrast to the experiments with simultaneous detection of the supercontinuum emission, conical emission, and plasma luminescence during filamentation, where interpretation of experimental results is often hindered, the above-mentioned technique implies investigation of the localisation of the light field responsible for the CC occurrence after recording the CC structures formed under filamentation [10–12].

When a LiF crystal is exposed to a train of pulses, the formation of long-lived CCs in it is accompanied by (i) an increase in the refractive index on the filament axis and the formation of an optical waveguide in the dielectric bulk and (ii) the occurrence of absorption bands [1, 10, 13, 14], which can significantly affect the supercontinuum formation. At the same time, the experiments with a multipulse exposure of LiF to near-IR (775 nm) pulses [4] did not reveal any influence of induced CCs on the supercontinuum spectrum and its generation efficiency.

In this context, we should note the following two circumstances. First, the experiments were performed in [4] in the regime of generation of a multifilament supercontinuum, with radiation power exceeding the critical self-focusing power by several orders of magnitude. In a number of important appli-

S.V. Chekalin, V.O. Kompanets Institute of Spectroscopy, Russian Academy of Sciences, ul. Fizicheskaya 5, Troitsk, 108840 Moscow, Russia; e-mail: chekalin@isan.troitsk.ru, kompanetsvo@isan.troitsk.ru;
A.E. Dormidonov, V.P. Kandidov Department of Physics, M.V. Lomonosov Moscow State University, Vorob'evy Gory, 119991 Moscow, Russia; e-mail: dormidonov@gmail.com, kandidov@physics.msu.ru

Received 12 December 2016
Kvantovaya Elektronika **47** (3) 259–265 (2017)
Translated by Yu.P. Sin'kov

cations, where supercontinuum radiation is used, in particular, to carry out 'pump–broadband probe' experiments (with accumulation and averaging of the signal from many pulses), the regime of a so-called single-filament supercontinuum is used, which provides a much smaller spread of the supercontinuum parameters from shot to shot than in the multifilament regime. In the single-filament regime, the excitation pulse power only slightly exceeds the critical self-focusing power. Second, the filamentation was investigated in [4] under the normal GVD conditions, and the question about the influence of the anomalous character of GVD on the supercontinuum under irradiation by mid-IR (near 3000 nm) pulses remained open.

In this paper, we report the results of an experimental study of the supercontinuum in LiF under filamentation of a train of pulses at wavelengths of 2600–3500 nm, i.e., in the region of strong anomalous GVD, at which the formation of single-cycle LBs was observed [11, 12]. The experiments were performed with pulses whose power only slightly exceeded the critical self-focusing power, which guaranteed the single-filament regime. The structures consisting of CCs, both induced by a single pulse and formed after multiple (up to several tens of thousands of mid-IR pulses) irradiation, and the supercontinuum spectra recorded under filamentation in these regimes were compared. An increase in the number of pulses forming a CC structure was found to cause a sharp drop of the intensity of the anti-Stokes wing in the UV range of the supercontinuum, up to its complete disappearance, and the generation of divergent supercontinuum radiation in the visible region.

2. Experimental setup

The experiments were performed using a laser radiation source based on a Tsunami femtosecond generator (Ti:sapphire laser) with a cw Millenia Vs solid-state pump laser, a Spitfire Pro regenerative amplifier with pumping by an Empower 30 pulsed solid-state laser, and a TOPAS-C tunable parametric amplifier with noncollinear generation at the difference frequency. The pulse FWHM was about 100 fs, and the spectrum half-width was 200–250 nm (depending on the pump wavelength). The pulse repetition rate varied from 1 kHz to the minimum value, corresponding to the single-pulse regime. The pulse energy, measured by a Fieldmax sensor with a PS-10 detector in the kHz range of the repetition frequency, reached 20 μJ. The pulse energy at a low repetition frequency was recorded by photo- and pyrometers, calibrated with respect to the PS-10 detector.

Laser pulses were focused by a thin CaF_2 lens with a focal length $F = 10$ cm into a LiF crystal 40 mm long at a distance of several millimetres from the crystal input face. To implement the single-filamentation regime, the pulse energy was varied from 10 to 18 μJ at a centre wavelength λ_0 varying from 2600 to 3500 nm, respectively. Under these conditions, in the case of single-pulse exposure, the sample was moved in the direction perpendicular to the laser beam axis after each pulse. In the case of multipulse exposure, a structure composed of CCs induced by many (500, 1000, or 10000) pulses was first formed at a low repetition rate (4 Hz) to exclude thermal effects, and then, without changing the sample position, the supercontinuum spectrum was measured under filamentation of several pulses (in a number sufficient for its detection). Thus, we investigated the influence of the structure consisting of CCs induced by different numbers of pulses on the supercontinuum.

A comprehensive analysis of the recorded CC structure was performed using an Euromex Oxion 5 microscope with illumination by a cw 450-nm laser and detection of luminescence by a Nikon D800 digital camera. The scattered excitation radiation was cut off by an auxiliary yellow-green light filter.

Spectra were recorded by an ASP-100MF fibre spectrometer and an ASPIRHS spectrometer (Avesta Ltd) in the spectral ranges of 200–1100 and 1200–2500 nm, respectively; a spectrometer based on a Solar Tii MS2004 monochromator and a pyroelectric detector was also used to detect mid-IR radiation. To obtain integral spectra of the anti-Stokes band in the supercontinuum, the divergent radiation was focused onto a diffuse scatterer, mounted directly before the spectrometer input.

The spectral–angular energy distribution for the anti-Stokes wing of the supercontinuum was measured by scanning the multimode fibre of the ASP-100MF spectrometer over the divergence angle of the supercontinuum. To this end, the fibre 400 μm in diameter was installed on a movable angular carriage with a radius of 50 mm and rotation centre located on the sample rear face. The supercontinuum image on a white (luminescent under UV irradiation) paper screen, installed at a distance of 100 mm from the sample rear face, was recorded by a Nikon D800 digital camera.

3. Experimental results

3.1. Luminescence of CC structures and their sizes

Figure 1 shows photographs of luminescence intensity distributions for the structures of CCs induced by a single pulse (top) and a train of 10 pulses (bottom) in LiF. The luminescence wavelengths (650 or 550 nm, depending on the intensity of the illuminating laser radiation [11]) and the occurrence of characteristic bands near 248 and 450 nm in the measured absorption spectrum of the structure induced in LiF by a train of 3100-nm pulses, confirm the occurrence of luminescent F_2 and F_3^+ centres and nonluminescent F centres [1, 10]. The modulation of luminescence intensity along the filament axis, corresponding to the change in the CC density with a characteristic period of about 30 μm (which depends on the IR pulse wavelength [11, 12]), is a manifestation of the periodic change in the maximum light field amplitude in the wave packet during its propagation in a dispersive medium. This effect is characteristic of only pulses with a duration close to the period of optical oscillations (single-cycle pulses) and is the result of the periodic change in the phase shift between the carrier wave and the wave packet envelope due to the difference in the group and phase veloc-

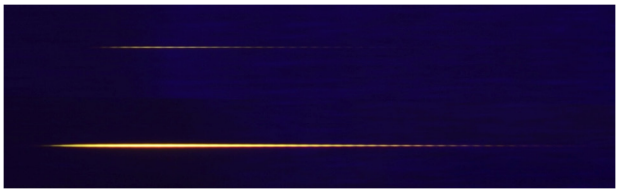

Figure 1. Longitudinal luminescence intensity profiles of the CC structures obtained after irradiation of a LiF crystal by one (top) and ten (bottom) pulses at λ_0 = 3100 nm. The modulation period along the structure axis is 31 μm.

ities [15]. Therefore, the observed modulation of the luminescence intensity is indicative of the formation of a single-cycle LB as a result of the compression of an IR pulse during its filamentation [11, 12].

This modulation can also be seen when irradiation is performed by a train of pulses; however, in this case, the modulation region is significantly shifted along the LB propagation path (to the filament tail) (Fig. 1, bottom). The structure is obscured in the region where the LB induced by a single pulse is recorded. The reason is the random displacement of the LB position at small fluctuations of the initial pulse energy. With an increase in the number of pulses, this pattern continues developing, a fact indicating that the CC structure (transparent in the mid-IR range), without being a hindrance for the occurrence of LBs, may even improve the conditions for the LB generation and propagation due to the formation of a waveguide [10, 14]. As a result, the LB formed by the next pulse passes a much longer path during its lifetime than the bullet formed by the preceding pulse. An increase in the number of pulses in a sequence forming CC structures makes these structures larger. Indeed, the structure length ranges from 0.5 to 1.2 mm (for wavelengths ranging from 2600 to 3500 nm), and the diameter is of the same order of magnitude as the wavelength [11] in the single-pulse regime, whereas after the exposure to 10 thousands of pulses the structure length exceeds 15 mm, and the diameter reaches several tens of micrometers (Fig. 2). The structure is mainly elongated at its output because of the waveguide character of the actuating pulse propagation [10]. Under these conditions, the modulation at the waveguide output arises more and more rarely, and the structure becomes completely homogeneous after exposure to several thousands of pulses.

The luminescence intensity distribution over the CC waveguide cross section contains a dip in the centre (Fig. 2), which is most likely related to the luminescence concentration quenching with an increase in the concentration of stored CCs. According to the data reported in [1], the observed decrease (by more than half) in the luminescence yield (Fig. 2) corresponds to the increase in the CC concentration to $\sim 10^{18}$ cm^{-3}. The same effect was observed for the luminescence from both types of CCs, F_2 and F_3^+ (at 650 and 550 nm, respectively), which is indicative of their equal concentrations in the structures formed.

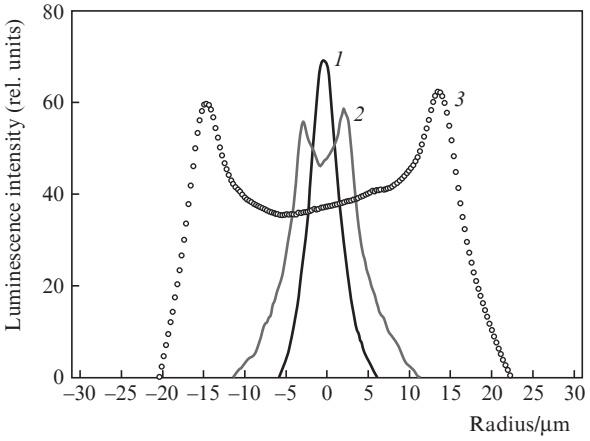

Figure 2. Transverse luminescence intensity profiles of the CC structures, obtained after irradiation of a LiF crystal by sequences of (*1*) 10, (*2*) 1000, and (*3*) more than 10000 pulses with $\lambda_0 = 3100$ nm.

3.2. Supercontinuum spectra

Figure 3 shows the normalised spectra of the anti-Stokes band in the supercontinuum, which were measured in a homogeneous LiF crystal in the case of the formation of one filament in a single pulse at different wavelengths in the mid-IR range. It can be seen that the anti-Stokes spectral band of the supercontinuum is narrowed with an increase in the pump wavelength from 1900 to 3300 nm and simultaneously shifts from the visible range to the UV region. At the same time, the conversion efficiency into this band decreases from $\sim 10^{-2}$ to less than 10^{-4}. To explain the short-wavelength shift, which was also observed for fused silica [16, 17], CaF_2, and BaF_2 [18], a dispersion equation was derived in [19] for the maximum of the anti-Stokes spectral band, and a general regularity determining the dispersion shift of the anti-Stokes band of supercontinuum was established.

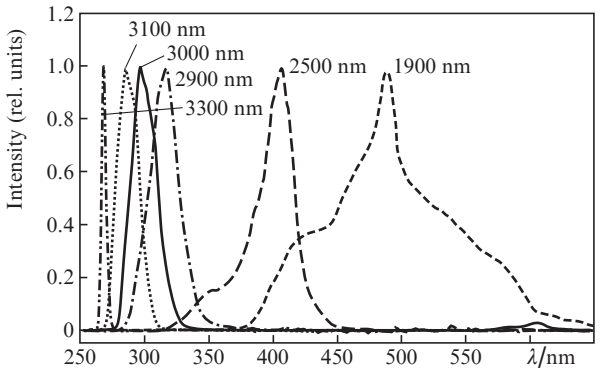

Figure 3. Normalised spectra of the anti-Stokes band of the supercontinuum, measured in a homogeneous LiF crystal at the formation of one filament in a single pulse at different wavelengths in the mid-IR range.

The spectral–angular distribution of the anti-Stokes wing of the supercontinuum for a single pulse at $\lambda_0 = 3100$ nm (Figs 3, 4a) contains only one narrow band (near 300 nm) of the radiation propagating along the filament axis. With an increase in the number of pulses, the intensity of this radiation sharply decreases and is slightly red-shifted with a simultaneous decrease in the spectral width (Fig. 5). In addition, weaker divergent rainbow rings arise in the supercontinuum spectrum for the CC structure induced by several hundreds of pulses (Figs 4b, 6b–6d). In contrast to the conical emission in the supercontinuum under femtosecond filamentation in the near-IR range, the divergence of the long-wavelength components of spectral rings in the visible region exceeds that of the short-wavelength components (8.5° at 600 nm and 6.5° at 420 nm, respectively). With an increase in the number of pulses forming the CC structure, the rainbow rings can be seen well on the distant screen (Fig. 6). Their occurrence is accompanied by the disappearance of blue luminescence on the axis, caused by the paper screen luminescence under irradiation by the UV light of the anti-Stokes wing of supercontinuum in the first pulses. The angular divergence of the radiation and its intensity barely change with an increase in the number of pulses to several thousands, and after the exposure to 10 thousands of pulses or more, the rings gradually disappear.

The wavelength of the pulses forming the CC significantly affects the characteristics of the frequency–angular supercontinuum spectrum under filamentation in the induced

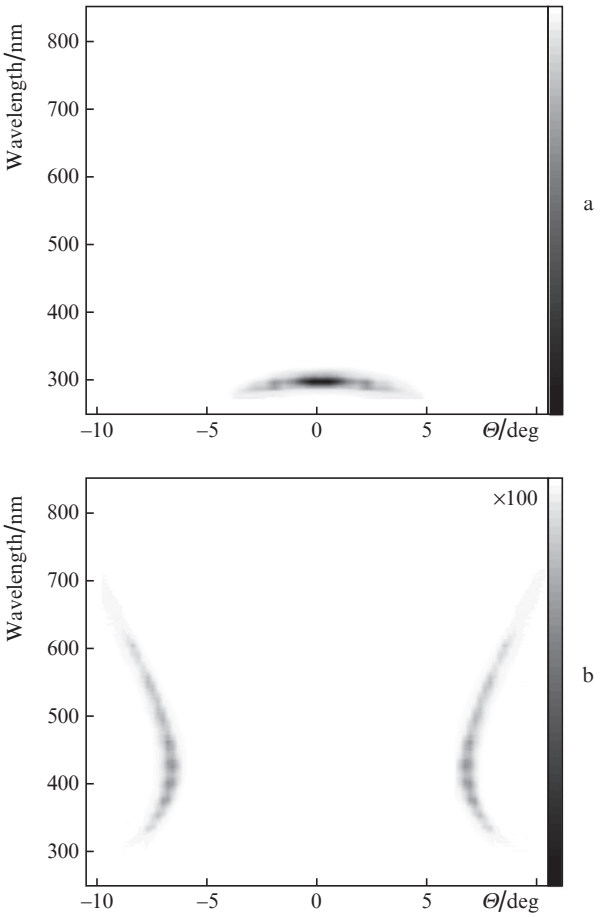

Figure 4. Spectral–angular distribution of the anti-Stokes wing of the supercontinuum (a) after irradiation of a LiF crystal free of CCs by a single pulse with $\lambda_0 = 3100$ nm and (b) after irradiation by 2000 pulses. The spectrum in panel (b) was recorded with an exposure larger than that in panel (a) by a factor of 100.

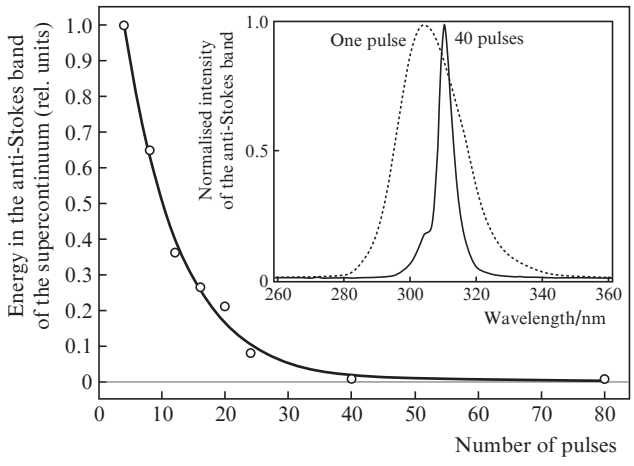

Figure 5. Dependence of the energy of the anti-Stokes wing of the supercontinuum on the number of pulses at $\lambda_0 = 3100$ nm in a LiF crystal. The inset shows the integral spectra of the anti-Stokes wing recorded after irradiation by one pulse and by 40 pulses, forming CCs.

structure. With a decrease in λ_0 to 2600 nm, the brightness of the rings essentially decreases, and the rates of their disappearance and the reduction in the energy of the anti-Stokes band slow down. The angular divergence of the entire ring

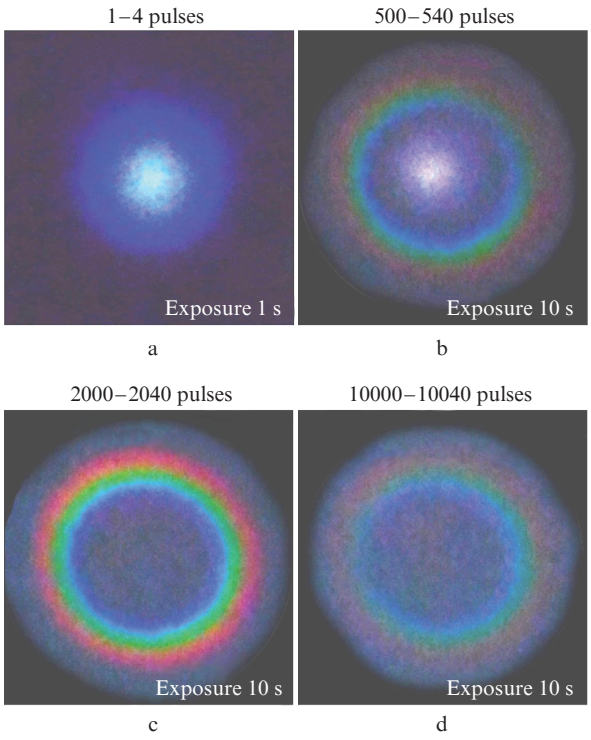

Figure 6. Supercontinuum images on a paper screen, obtained with an increase in the number of pulses forming CCs. The pulse repetition rate is 4 Hz. The photographs were made (a) during the first four pulses and (b, c, d) during 40 pulses after irradiating the sample with (b) 500, (c) 2000, and (d) 10000 pulses.

structure increases (to 9° at 420 nm). At the same time, the energy fraction in the anti-Stokes band, recorded under single-pulse filamentation, rises to 0.4% from the value of less than 0.01% measured at a wavelength of 3100 nm. Under filamentation of 3500-nm pulses, the energy fraction in the anti-Stokes band becomes so small that cannot be observed on the paper screen.

The supercontinuum spectrum recorded near the actuating pulse wavelength (Fig. 7), in contrast to the anti-Stokes wing,

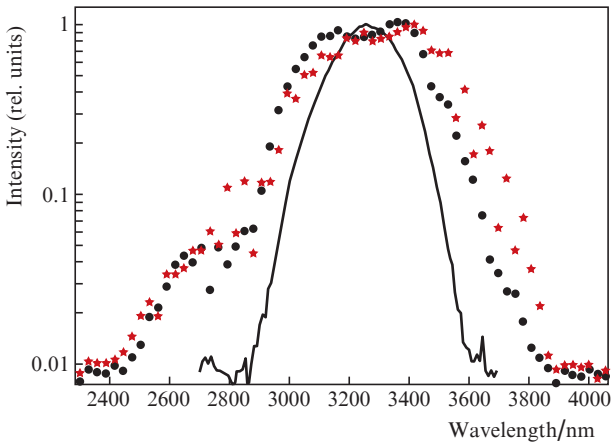

Figure 7. Normalised supercontinuum spectra, recorded near the actuating pulse wavelength (3250 nm): (solid curve) spectrum of the initial pulse, (asterisks) supercontinuum spectrum of a single pulse in the absence of CCs, and (circles) supercontinuum spectrum recorded after CC accumulation (~2000 pulses).

does not undergo any significant changes under filamentation in a LiF crystal free of CCs and in a crystal with a structure induced by many pulses: in both cases one can observe an approximately twofold broadening in comparison with the initial spectrum of the actuating pulse and the occurrence of a dip in the centre, which is characteristic of the spectrum of single-cycle pulses [20]. Thus, after the exposure to 10000 pulses, which form well-developed long-lived CC structures, the supercontinuum spectrum of the LB contains only one broadened band in the mid-IR range, in contrast to the single-pulse filamentation in the absence of CCs, a case where the spectrum contains, along with this band, a rather strong anti-Stokes wing.

4. Numerical simulation

The theoretical study of the influence of induced CCs on the LB formation and propagation was based on a numerical simulation of the laser pulse filamentation in the LiF crystal. The simulation used the approximation of a slowly varying envelope [15], which adequately describes wave packets with durations up to those comparable with the optical oscillation period. When formalising this problem, we took into account the wave packet diffraction and dispersion, Kerr self-focusing, photoionisation and avalanche ionisation of the medium, defocusing and absorption of light in the induced plasma, and the effect of pulse self-steepening [12]. The material dispersion of LiF was calculated from the Sellmeier formula, and the photoionisation rate was determined using the Keldysh formalism [21]. The CCs induced in the medium were taken into account in the form of a model of extended waveguide with a refractive index profile corresponding to that presented in Fig. 2 (curve *1*). According to the experimental data of [1], the maximum increment in the refractive index on the waveguide axis is $\Delta n_{WG} = 0.01$. The waveguide coordinate z_{WG} corresponded to the filamentation start, i.e., the point at which pronounced photoionisation of the medium (and, therefore, CC formation) began.

We considered a pulse with parameters corresponding to experimental: centre wavelength of 3100 nm; duration of 100 fs (at half maximum); and energy of 15 μJ, which corresponds to a peak power of about $1.5P_{cr}$ (P_{cr} is the critical power of self-focusing in LiF).

The calculated intensity distribution $I(r,\tau)$ for the pulse light field at a distance of $z = 7.26$ mm from the input face of the crystal is shown in Fig. 8a in the local frame of reference of the pulse: $\tau = t - z/v_g$, where v_g is the pulse group velocity. The beginning of the waveguide was located at the point $z_{WG} = 7.05$ mm; i.e., the LB formed in the waveguide passed a distance of about 0.2 mm. It can be seen that, after entering the waveguide, the bullet frontal part was localised in correspondence with the specified gradient of the refractive index. However, the intense part of the LB is a stable formation, insensitive to the waveguide parameters. The reason is that the nonlinear additive to the refractive index $n_2 I$ becomes comparable with the CC-induced increment Δn_{WG}. For com-

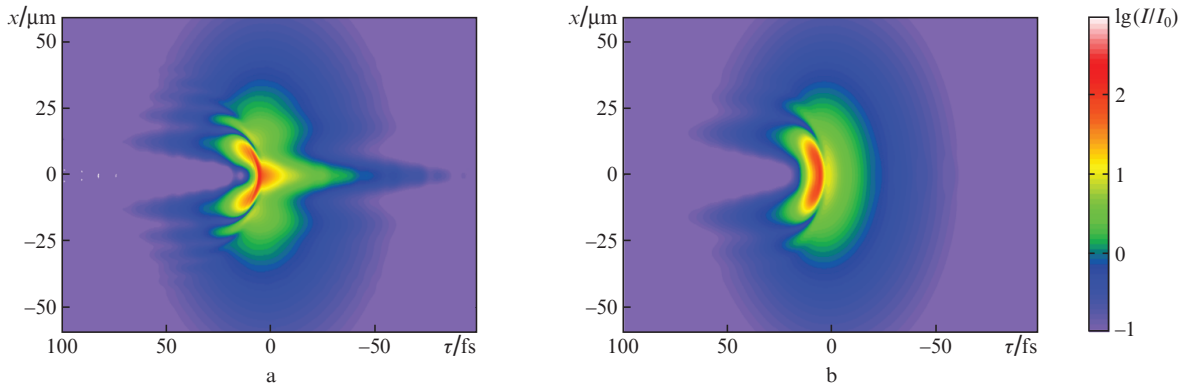

Figure 8. Spatial and temporal intensity distribution $I(r,\tau)$ in LBs at $z = 7.26$ mm (a) in the case of CC-induced change in the refractive index and (b) in the case of free propagation.

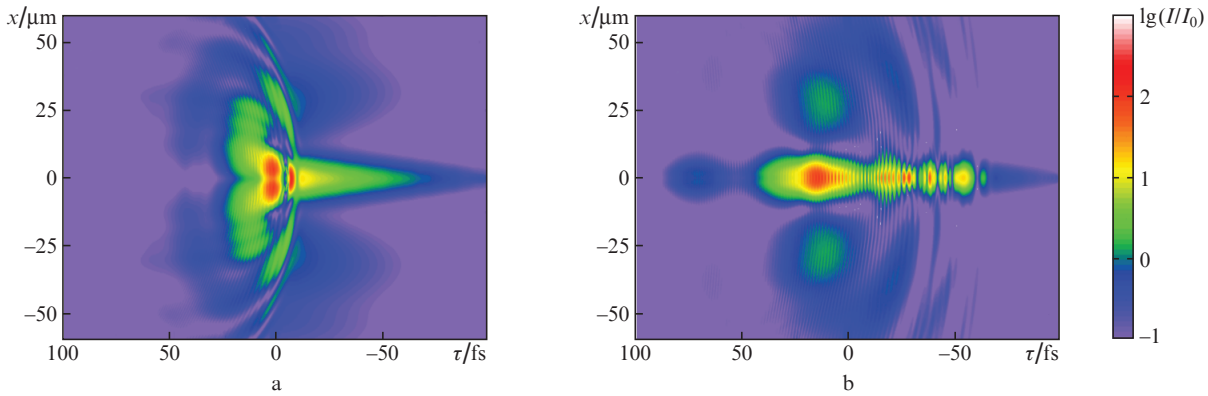

Figure 9. Multifocus structure of the LB propagating in a waveguide at distances of $z \approx$ (a) 7.5 and (b) 8.5 mm.

parison, Fig. 8b shows the pulse intensity distribution $I(r,\tau)$ for free LB propagation. In this case, the pulse frontal part is not localised, and the shape of the intense region is practically the same as for the LB in the waveguide propagation regime.

The fundamental feature of the LB waveguide propagation regime manifests itself in the energy localisation in the frontal part of the pulse. In this case, the second nonlinear focus is formed at a distance of $z \approx 7.5$ mm. The intensity of the new formation becomes sufficiently high to photoionise the medium and defocus the main LB, located at the pulse centre (Fig. 9a). The formation of nonlinear points is successively repeated at different distances z (Fig. 9b). As a result, the pulse acquires a complex multifocus structure. The plasma arising in each newly formed focus leads to defocusing of the radiation following behind. This pattern is not observed in the free propagation regime.

Thus, the existence of the waveguide formed by induced CCs significantly increases the LB path length. The pulse filamentation in the waveguide under anomalous GVD conditions leads to the formation of a sequence of nonlinear foci. It is noteworthy that an extended filament is formed in a pulse whose peak power only slightly exceeds the critical power of self-focusing. The numerical simulation results are in agreement with the experimentally recorded increase in the length of the CC structure with an increase in the number of incident pulses (see Fig. 1).

5. Discussion of the results

The formation of a waveguide in LiF, which increases the LB path length, is one of the reasons for the observed decrease in the anti-Stokes wing energy with an increase in the number of waveguide-forming pulses (see Figs 4–6). Indeed, the anti-Stokes broadening of the supercontinuum spectrum occurs as a result of the self-phase modulation of the pulse tail light field under the conditions of a strong negative intensity gradient in time, which is due to sharp defocusing in the induced laser plasma and self-sharpening of the trailing edge of its envelope [22]. The destructive interference of the supercontinuum radiation emitted by the LB leads (under the anomalous GVD conditions) to the formation of a wide minimum between the wavelength range of the incident pulse and the anti-Stokes band. An isolated anti-Stokes wing is formed as a result, in which the supercontinuum spectral intensity is lower than at the actuating pulse wavelength by a factor of about 30 but is several orders of magnitude higher than that in the newly formed minimum [16]. These regularities in the frequency–angular supercontinuum spectrum are observed in different dielectrics during femtosecond filamentation under anomalous GVD conditions [17, 18, 21–25] and in LiF in the absence of induced CCs (Fig. 3). With an increase in the LB path length due to the waveguide formation, the destructive interference range in the supercontinuum is expanded, the spectral band of the anti-Stokes wing narrows, and its energy decreases. The sharp decrease in the anti-Stokes wing energy with increasing incident pulse wavelength, which was observed in our experiments, can also be related to the rise in the CC structure length (and, therefore, the LB path length), which was revealed by laser colouration [11].

Another reason for a decrease in energy and a shift of the anti-Stokes band of the supercontinuum, observed under filamentation of pulses in LiF with CCs (see Fig. 5), is the absorption and scattering of a broadband supercontinuum by the CC structure. While the structure is elongated with an increase in the number of incident pulses, the wide absorption lines at 248 and 450 nm, recorded in the samples under study, significantly weaken the anti-Stokes radiation of the supercontinuum. The scattering of this radiation with a wavelength λ from a periodic structure formed by induced CCs can be estimated using a simple relation for the spectral intensity of scattered radiation:

$$S(\lambda,\theta) \propto \left[\frac{\sin(N\Delta\phi/2)}{\sin(\Delta\phi/2)}\right]^2,$$

where $\Delta\phi = 2\pi d(1 - \cos\theta)/\lambda$ is the phase shift of the supercontinuum radiation scattered from neighboring inhomogeneities, d is the structure period, θ is the scattering angle, and N is the number of inhomogeneities in the structure. Hence, $\theta \approx \sqrt{2\lambda/d}$, i.e., the scattering angle increases with increasing wavelength λ of the supercontinuum radiation; this behaviour is consistent with the experimental results (Figs 4, 6). At $\lambda = 420$ nm, the angle θ in the case of supercontinuum radiation scattering in a structure with a period $d = 31$ μm is about 9° and increases to 11° at $\lambda = 600$ nm. These estimates are close to the experimental data (Fig. 4). The increase in the divergence of the entire colour ring with a decrease in the excitation wavelength to 2600 nm is apparently caused by the reduction in the diameter of the induced waveguide and the corresponding rise in the diffraction divergence of the radiation emerging from it.

6. Conclusions

The frequency–angular spectrum of supercontinuum, generated by a mid-IR LB, is determined by many factors. The occurrence of the waveguide propagation mode for LB due to the formation of stable CCs in a LiF crystal as a result of the multipulse femtosecond filamentation radically changes the formation scenario for the frequency--angular spectrum. First, the LB path length increases in the waveguide, which leads to expansion of the destructive interference region and, as a consequence, to a blue shift, spectral band narrowing, and decrease in the intensity of the anti-Stokes wing in the supercontinuum. Second, the absorption at wavelengths of 248 and 450 nm in the induced CCs weakens the anti-Stokes band, as a result of which weak radiation arises in the visible range (in the destructive interference region). The angular divergence of this radiation is determined by the effects of scattering from the inhomogeneous structure of the induced CC waveguide. Thus, the modification of the medium under multipulse filamentation in lithium fluoride affects significantly the formation of the LB and its frequency–angular supercontinuum spectrum in the femtosecond radiation of the mid-IR range.

Acknowledgements. This work was supported by the Russian Foundation for Basic Research (Grant Nos 14-22-02025-ofi_m and 15-32-50193-mol_nr), the RF President's Grants Council (Support to the Leading Scientific Schools Programme, Grant No. 9695.2016.2), and the Presidium of the Russian Academy of Sciences (Programme 'Extreme laser radiation: physics and fundamental applications').

References

1. Baldacchini G. *J. Luminescence*, **100**, 333 (2002).
2. Brodeur A., Chin S.L. *J. Opt. Soc. Am. B*, **16**, 637 (1999).

3. Tzankov P., Buchvarov I., Fiebig T. *Opt. Commun.*, **203**, 107 (2002).
4. Kohl-Landgraf J., Nimsch J.-E., Wachtveitl J. *Opt. Express*, **21**, 17060 (2013).
5. Stuart B.C., Feit M.D., Rubenchik A.M., Shore B.W., Perry M.D. *J. Opt. Soc. Am. B*, **13**, 459 (1996).
6. Kaiser A., Rethfeld B., Vicanek M., Simon G. *Phys. Rev. B*, **61**, 11437 (2000).
7. Mao S.S., Quéré F., Guizard S., Mao X., Russo R.E., Petite G., Martin P. *Appl. Phys. A*, **79**, 1695 (2004).
8. Lushchik Ch.B., Lushchik A.Ch. *Raspad elektronnykh vozbuzhdenii s obrazovaniem defektov v tverdykh telakh* (Decay of Electronic Excitations with Formation of Defects in Solids) (Moscow: Nauka, 1989).
9. Hirai M., Suzuki Y., Okumura M. *J. Phys. Colloques*, **41**, C6-305 (1980).
10. Martynovich E.F., Kuznetsov A.V., Kirpichnikov A.V., Pestryakov E.V., Bagaev S.N. *Quantum Electron.*, **43**, 463 (2013) [*Kvantovaya Elektron.*, **43**, 463 (2013)].
11. Kuznetsov A.V., Kompanets V.O., Dormidonov A.E., Chekalin S.V., Shlenov S.A., Kandidov V.P. *Quantum Electron.*, **46**, 379 (2016) [*Kvantovaya Elektron*., **46**, 379 (2016)].
12. Chekalin S.V., Kompanets V.O., Kuznetsov A.V., Dormidonov A.E., Kandidov V.P. *Laser Phys. Lett*., **13**, 065401 (2016).
13. Cheng G., Wang Y., He J.F., Chen G., Zhao W. *Opt. Express*, **15**, 8938 (2007).
14. Chiamenti I., Bonfigli F., Montereali R.M., Kalinowski H. *J. Microwaves, Optoelectron. Electromagn. Applicat.*, **13**, 47 (2014).
15. Brabec T., Krausz F. *Phys. Rev. Lett.*, **78**, 3282 (1997).
16. Smetanina E.O., Kompanets V.O., Chekalin S.V., Dormidonov A.E., Kandidov V.P. *Opt. Lett*., **38**, 16 (2013).
17. Durand M., Lim K., Jukna V., McKee E., Baudelet M., Houard A., Richardson M., Mysyrowicz A., Couairon A. *Phys. Rev. A*, **87**, 043820 (2013).
18. Dormidonov A.E., Kompanets V.O., Chekalin S.V., Kandidov V.P. *Opt. Express*, **23**, 29202 (2015).
19. Dormidonov A.E., Kompanets V.O., Chekalin S.V., Kandidov V.P. *Pis'ma Zh. Eksp. Teor. Fiz.*, **104**, 173 (2016).
20. Fan G., Balciunas T., Fourcade-Dutin C., Haessler S., Voronin A.A., Zheltikov A.M., Gérôme F., Benabid F., Baltuška A., Witting T. *Opt. Express*, **24**, 12713 (2016).
21. Keldysh L.V. *Zh. Eksp. Teor. Fiz.*, **47** (5), 1945 (1964).
22. Kandidov V.P., Kosareva O.G., Golubtsov I.S., Liu W., Becker A., Akozbek N., Bowden C.M., Chin C.L. *Appl. Phys. B*, **77**, 149 (2003).
23. Dharmadhikari J.A., Deshpande R.A., Nath A., Dota K., Mathur D., Dharmadhikari A.K. *Appl. Phys. B*, **117**, 471 (2014).
24. Vasa P., Dharmadhikari J.A., Dharmadhikari A.K., Sharma R., Singh M., Mathur D. *Phys. Rev. A*, **89**, 043834 (2014).
25. Jukna V., Galinis J., Tamošauskas G., Majus D., Dubietis A. *Appl. Phys. B*, **116**, 477 (2014).